

RESEARCH

Open Access



# Evaluation of commonly used reinforcement materials for color paintings on ancient wooden architecture in China

Kezhu Han<sup>1</sup>, Gele Teri<sup>1</sup>, Cong Cheng<sup>1</sup>, Yuxiao Tian<sup>1</sup>, Dan Huang<sup>1</sup>, Mantang Ge<sup>1</sup>, Peng Fu<sup>2\*</sup>, Yujia Luo<sup>1\*</sup> and Yuhu Li<sup>1\*</sup>

## Abstract

Over recent decades, various heritage institutions have utilized a multitude of materials to reinforce the painted layers of ancient Chinese wooden architecture. In this study, we conducted a comprehensive evaluation of the properties and durability of four widely used reinforcement agents, i.e., AC33, B72, FKM, and FEVE, using a series of techniques, including contact angle tests, water vapor permeability measurements, color difference evaluations, tensile strength tests, UV-vis spectrometry, and scanning electron microscopy (SEM). The results demonstrate that the transmittance rates of the films made from these four reinforcement agents are approximately 100% in the visible light range. Among them, the B72 film exhibits the highest hydrophobicity. The AC33 film has better permeability, fair tensile strength, and is more hydrophilic. FKM film is more hydrophobic but has lower permeability and tensile strength. Overall, the FEVE film presents the best comprehensive properties, including better hydrophobicity, higher permeability, and tensile strength. This research provides data evidence to guide heritage conservators and curators in decision-making when selecting appropriate reinforcement materials in practice.

**Keywords** Color painting, Evaluation, Reinforcement agents

## Introduction

Ancient Chinese architecture stands out in the history of world architecture not only for its unique styles but also for its vibrant and intricate decorative paintings [1–3]. These paintings are distinctive features of ancient Chinese architecture, embodying rich ethnic traits and great

cultural significance [4]. Typically, these decorative paintings comprise three layers, i.e., the painted layer or the pigment layer, the mortar (or ‘Di Zhang’) layer, and the wooden layer, as shown in Fig. 1a and b. The wooden layer refers to the fundamental structure of ancient buildings, the mortar layer conceals the patterns of the wooden surface, such as scars, stains, uneven textures, and color inconsistencies, and provides support for the subsequent painting. This layer is commonly made of mixed materials including brick dust, tung oil [5], flour [6], lime, pig blood [7], and ramie fibers [6], according to specific ratios (Fig. 1c). The painted layer, made from mixed pigment powders and different types of gules, such as animal glue [8], gelatin [9], and fish glue [1], serves to decorate the architecture, and some toxic pigments can prevent architecture from insect infestations, e.g., cinnabar, red lead, and Paris green [1].

\*Correspondence:

Peng Fu  
fupeng@snnu.edu.cn  
Yujia Luo  
yujialuo@snnu.edu.cn  
Yuhu Li  
liyuhu@snnu.edu.cn

<sup>1</sup> Engineering Research Center of Historical Cultural Heritage Conservation, Ministry of Education, School of Materials Science and Engineering, Shaanxi Normal University, Xi’an 710119, Shaanxi, China  
<sup>2</sup> Shaanxi Institute for the Preservation of Culture Heritage, Xi’an 710119, Shaanxi, China



© The Author(s) 2024. **Open Access** This article is licensed under a Creative Commons Attribution 4.0 International License, which permits use, sharing, adaptation, distribution and reproduction in any medium or format, as long as you give appropriate credit to the original author(s) and the source, provide a link to the Creative Commons licence, and indicate if changes were made. The images or other third party material in this article are included in the article's Creative Commons licence, unless indicated otherwise in a credit line to the material. If material is not included in the article's Creative Commons licence and your intended use is not permitted by statutory regulation or exceeds the permitted use, you will need to obtain permission directly from the copyright holder. To view a copy of this licence, visit <http://creativecommons.org/licenses/by/4.0/>. The Creative Commons Public Domain Dedication waiver (<http://creativecommons.org/publicdomain/zero/1.0/>) applies to the data made available in this article, unless otherwise stated in a credit line to the data.

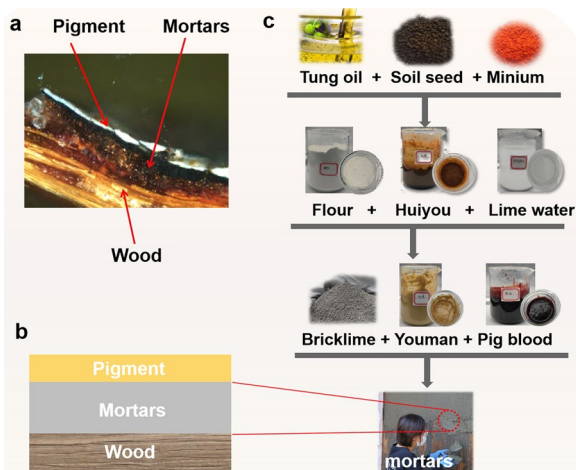


**Fig. 1** a Cross-section of decorative paintings on ancient Chinese architecture; b cross-section structure diagram of the decorative paintings; c composition of the mortar layer

As shown in Fig. 1, various raw materials used in mortar production can degrade over time, vulnerable to damage from external environmental factors [10, 11]. Fluctuations in temperature and humidity, along with long-time exposure to sunlight radiation, directly affect the durability of the color paintings, causing issues like fading, peeling, cracking, powdering, detachment, and in extreme cases, the total loss of the painted layer. In recent decades, several materials have been employed by heritage institutions for reinforcement of the painted layer for paintings on the ancient wooded architectures in practices, e.g., Paraloid B-72 [12], Acrylic resin Primal AC33 [13–15], polyvinyl acetate (PVAc) emulsion [16], waterborne epoxy [17], fluoroelastomer (FKM) [18–20], trifluoro vinyl chloride and vinyl ether copolymer (FEVE fluorocarbon resin) [21], tung oil, and modified gelatin. However, some of the reinforcement agents

can themselves degrade [14, 22, 23] and potentially exacerbate damage to the painted layers [24, 25]. Paraloid B-72, popular for its transparency and strong adhesion to pigments, does not alter the appearance or optical properties of heritage items. Nevertheless, the B72 film can reduce the permeability of the objects [26], and lead to film discoloration over time [27]. Alternatives, such as fluorinated polymers [28, 29], the mixture of acrylic and fluorinated polymers [30, 31], and the mixture of silanes and siloxanes [32], the mixture of Paraloid B72 and boric acid [33], nanohydroxides [34], began to be used, but each presents its drawbacks. Also, curators tend to use traditional materials, such as gelatin and bone glue, which are consistent with original materials for conservation treatments [35, 36]. The tung oil has been tried to be applied for painting reinforcement, while it takes a few years to completely dry, during which it absorbs dirt in the air, often leading to surface darkening.

Most of the currently available studies have focused on evaluating the immediate reinforcing effects of materials on treated sections of decorative paintings [13, 21], there is a knowledge gap in the systematic characterization and exploration of durability for the reinforcing agents. This study aims to bridge this gap by investigating the effectiveness of the most commonly used reinforcing materials on various pigments in China. Specifically, according to reported studies as summarized in Table 1 and preliminary in-situ investigation (Fig. 2), the most commonly used four types of reinforcing agents, employed by different Chinese heritage institutions, were selected for a comprehensive evaluation in this research. For example, according to previous conservation recordings provided by curators, B72 was executed on the color paintings in the Puren Temple (Hebei province) in 2013 (Fig. 2a<sub>1</sub> and a<sub>2</sub>), FEVE and AC33 were used to reinforce the paintings in the Qianlong Garden (Fig. 2b<sub>1</sub> and b<sub>2</sub>), and the paintings in the East Prosperity Gate (Fig. 2c<sub>1</sub> and c<sub>2</sub>) in the

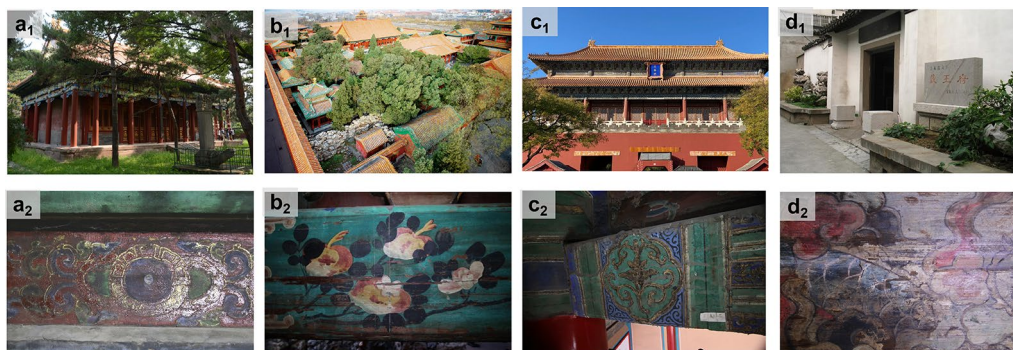


**Fig. 2** The preliminary in-situ investigation of the reinforcing agents for color paintings in four different heritage sites. a<sub>1</sub>, a<sub>2</sub>: the color painting in the Puren temple; b<sub>1</sub>, b<sub>2</sub>: the color painting in the Qianlong Garden in the Palace Museum; c<sub>1</sub>, c<sub>2</sub>: the color painting in the east Prosperity Gate in the Palace Museum; d<sub>1</sub>, d<sub>2</sub>: the color painting in the Taiping Heavenly Kingdom Prince Dai's mansion

**Table 1** A summary of the use of reinforcing agents for the color paintings on ancient wooden architecture in China

Institutions	Architecture	Paint layer reinforcement reagents
China Academy of Cultural Heritage	Luoyang Shaanxi Guild Hall (2004) [37]	5–20% Acrylic resin Primal (AC33) or 2–5% Paraloid B-72
	Puren Temple (2011)	2–5% Paraloid B-72
Shaanxi Institute for the Preservation of Cultural Heritage	Tianshui Fuxi Temple Congenital Hall (2005)	2% Paraloid B-72
	The Palace Museum Zhendu Gate (2005)	3%, 5%, 10% Paraloid B72
Nanjing Museum	Dacheng Hall of Confucius Temple, Hangzhou (2006)	Fluorelastomer
	Temple of Literature in Hangzhou (2007)	Fluorelastomer
	Jintan Dai Palace, Jiangsu Province (2013)	Fluorelastomer
	Grand Canal Yangzhou Yanzong Temple (2018) [18]	1–2% gelatin
The Palace Museum	East Prosperity Gate of the Palace Museum (2014)	5–20% Acrylic resin Primal (AC33)
	Qianlong Garden of the Palace Museum (2019)	3% FEVE fluorocarbon resin

Palace Museum (Beijing) in 2019 and 2012 respectively. FKM was applied to the paintings of Taiping Heavenly Kingdom Prince Dai's Mansion (Jiangsu province) in 2013, as shown in Fig. 2d<sub>1</sub> and d<sub>2</sub>. Currently, the reinforced painted layers using FEVE, AC33, and FKM demonstrate quite a small number of flaking pigments, and the reinforced color painting using B72 shows strong reflection to light (Fig. 2a<sub>2</sub>).

## Experiment section

### Preparation of the reinforcement reagents

5% (w/v) of Paraloid B72 granules (Acetone Chemical Reagent Co., Ltd., Beijing, China) was prepared by dissolving them in acetone, denoted as B72. A 3% fluorocarbon resin solution (Dalian Zhenbang Co., Ltd. Dalian, China) was prepared and labeled as FEVE. The fluorelastomer granules, obtained from Acetone Chemical Reagent Co., Ltd., Beijing, China, were dissolved in 3% methyl alcohol at 35 °C. This solution was then combined with butyl acetate in a 1:1 ratio, producing a mixture labeled as FKM. 3% acrylic resin primal AC33 (composed of 40% methyl methacrylate and 60% ethyl acrylate), provided by the Palace Museum, Beijing, China, was used directly and labeled as AC33.

### Preparation of films

The B72, FEVE, AC33, and FKM solutions were cast onto 76 × 26 mm microscope slides for air-drying under room conditions for 12 h and were used for all characterization but the mechanical tests. Given that not all of the films could be well taken off from the slides, the four reinforcing agents were also evenly coated onto Xuan paper, a homogenous, high-quality traditional Chinese paper [38], to evaluate the tensile strength of the reinforcement films.

### Preparation samples

The mortar layer was prepared by mixing the tung oil, flour, lime, and brick ash (provided by the Palace Museum) according to the ratios of the traditional recipe (as shown in Fig. 1a). This mixture was uniformly applied onto the 5 × 14.5 cm wooden boards (Fig. 3a) and air-dried under room conditions (25 °C, 50% RH) for 30 days (Fig. 3b). Six types of commonly used pigment powders with the same particle size (ultramarine, cinnabar, realgar, lead white, Paris green, and graphite), purchased from Beijing Tianya Pigment Co., Ltd. Beijing, China, were dissolved in 5% (w/v) gelatin solution respectively. These solutions were then evenly applied onto the mortar layer using brushes (Fig. 3c). Subsequently, these model samples were air-dried under room conditions for one week.

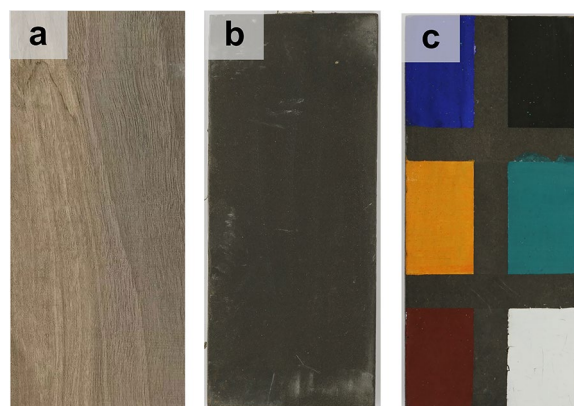


**Fig. 3** Model painting samples. **a** the wood support; **b** the mortar layer applied to the wood; **c** six types of pigments (ultramarine, cinnabar, realgar, lead white, Paris green, graphite) applied to the surface of the mortar layer

### The degradation of reference samples

Given that the pigments on the paintings have been being exposed to continuous outdoor sunlight and fluctuating temperature and relative humidity, leading to flaking of the pigments layer [39], the stability of the four reinforcing materials was evaluated under uncontrolled temperature and humidity conditions but with UV radiation exposure. Artificially UV degradation was performed using a UVB lamp of 180 W at 340 nm (OSRAM Co., Ltd., China) for 120 h at 10 cm distance in parallel to the films coated on slides and model painting samples.

### Characterization methods

#### Contact angle test

The video optical contact angle tester (Dataphysics, OCA20, Stuttgart, Germany) was used to take photos of water droplets, and 2  $\mu$ L of water was contained in the deposition drop. The droplet velocity is 1.635 mm/s, and the CCD inclination is 30°. The contact angle was measured on five different spots of the films (the films of B72, FEVE, AC33, and FKM), and average values were obtained and used.

#### Ultraviolet near-infrared spectrometer

UV–vis near-infrared spectrophotometer (PerkinElmer, Lambda 950, USA) was used to collect transmittance (%) of the four films across wavelengths ranging from 250 to 800 nm.

#### Water vapor transmission property

The water vapor transmission properties were explored for the four reinforcement agents in compliance with the standard ISO 12572:2016 with some modifications. Each agent was uniformly applied to model painting samples and left to air drying for 12 h. The coated surfaces of these model painting samples were then positioned over the opening of a collecting bottle, containing 100 mL of deionized water. The interface between the model painting samples and the bottle was securely sealed using Vaseline to prevent any external airflow. Subsequently, this entire setup was placed in an oven and dried at 35 °C for 21 days. To ascertain the effectiveness of the reinforcement agents in terms of water vapor permeability, the weight of the assembly was measured before and after the drying process. This procedure was repeated four times, and the average as calculated.

#### Mechanical characterization

The tensile strength was measured 10 times for each type of reinforced paper sample (15  $\times$  1.5 cm) using a universal testing machine (QT-1136PC, Guangzhou, China) with the tensile speed at 10 mm/min, and the average data were used for analysis. This strain rate was chosen due

to that it was difficult to test the brittle samples at higher strain rates.

#### Scanning electron microscope

Surface morphology of the film samples and model painting samples were observed using the scanning electron microscope (SEM, HITACHI SU3500, Japan), with a high-performance silicon drift detector and X-ray tube (Rh target); the test range was 11NA–92U. All samples were sprayed with gold for 120 s.

#### Colorimetric measurements

The CIE LAB system was used to evaluate the color changes of the same spot on the model painting samples before and after UV degradation following the equation [40, 41]

$$\Delta E = \sqrt{(\Delta L)^2 + (\Delta a)^2 + (\Delta b)^2}$$

where  $\Delta E$  is the color difference,  $\Delta L$ ,  $\Delta a$ , and  $\Delta b$  denotes lightness change, the degrees of difference in red and green and the degrees of difference in yellow and blue respectively. This measurement was conducted three times, and the average data were used for analysis.

#### Pencil hardness test

The pencil hardness test is a method for determining the film hardness by moving the pencil tips of known hardness over the coating at an angle of 45° to the horizontal with a force of 7.5 N. The test results are graded with 17 scales of 9B, ..., B, HB, F, H, ..., and 9 H of hardness, where 9B and 9H represent the softest and the hardest surface hardness, respectively based on the standard ISO 15184:2012(E).

## Results and discussion

### Properties of the films prepared using the four reinforcing agents

As shown in Fig. 4a, prior to film formation, the AC33 and FEVE solutions appear white and milky, whereas the B72 and FKM solutions are transparent. After the film formation, both AC33 and FKM films exhibit a smooth surface (Fig. 4b and e), in contrast to the B72 and FEVE films (Fig. 4c and d), which display a few surface bubbles. These bubble-like spots on the B72 and FEVE films are believed to result from phase invasion effects following solvent evaporation [42]. The highly flat surface of AC33 and FKM indicates that the material expands evenly during film formation.

It is acknowledged that a lower contact angle on a film surface indicates greater surface energy, leading to the film surface being contaminated by environmental conditions, such as rainwater, bird droppings, spider webs, etc.



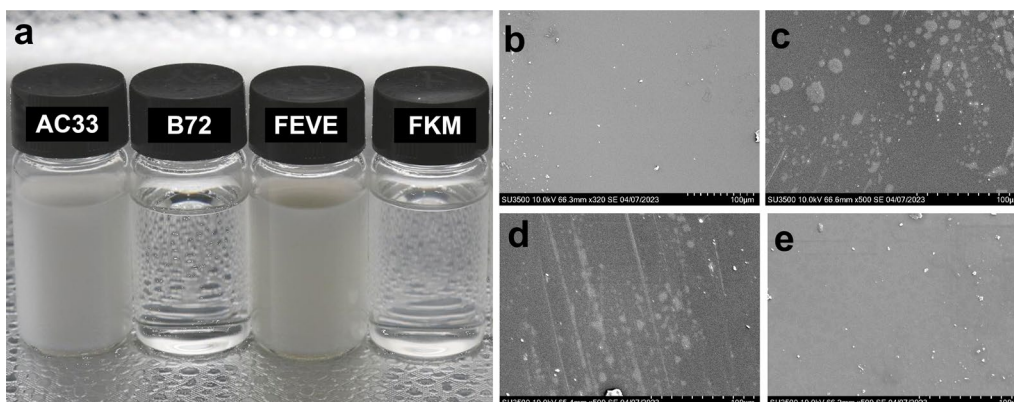


**Fig. 4** a The image of four reinforcement agents; b–e the SEM images of four reinforcement films made from the agents (AC33, B72, FEVE, and FKM)

[43, 44]. In Fig. 5a, contact angles of the film surface of AC33, B72, FEVE, and FKM are 58.74°, 74.24°, 63.73°, and 78.75° respectively after water drop maintaining for 90 s, where the data are in line with the results of reported studies [14, 45]. After 120-h UV degradation for the four films, the films leads to increasing surface roughness and decreasing contact angles [45], where contact angles of AC33, B72, FEVE, and FKM films decreased by 37.32%, 10.9%, 4.63%, and 6.73% respectively. This demonstrates that AC33 film with the highest surface energy, degrades at the highest rate among all reinforcement materials. The FEVE and FKM films have the lowest degradation rates in this test, showing relatively better stability.

To explore the effects of the four reinforcing films on the optical properties of the paintings, an excitation light source of 580 nm was used to evaluate the film transmittance (Fig. 5b). The transmittance rates for AC33, B72, FEVE, and FKM films were found to be approximately 100% across the visible light spectrum, ranging from 320 to 700 nm, which is in line with reported results, i.e.,

AC33 (99.26%) [13, 21], B72 (99.06%), FEVE (96.47%) [13, 21], FKM (97%) [46], suggesting that all films might not affect the morphology and optical properties of paintings.

Mechanical properties of the four reinforcement materials were explored by conducting pencil hardness test [47–49] for films dried on glass slides and tensile strength test for reagents dried on Xuan paper, to evaluate the surface stiffness of the films and film strength respectively, the results are shown in Table 2. As shown in Table 2, the B72 film exhibited the highest stiffness at 2H, while both AC33 and FKM films showed the lowest stiffness at HB. FEVE film has moderate stiffness at F. After UV degradation, the stiffness of B72, FEVE, and FKM films has decreased by one grade, while that of AC33 presents two-grade reduction. Also, B72 has the largest tensile strength at 15.89 MPa, which decreased by 18.94% following UV exposure, indicating superior mechanical properties compared to AC33, FEVE, and FKM, which showed decreases of 21.5%, 17.71%, and 24.63%, respectively. However, it’s important to note that excessive strength

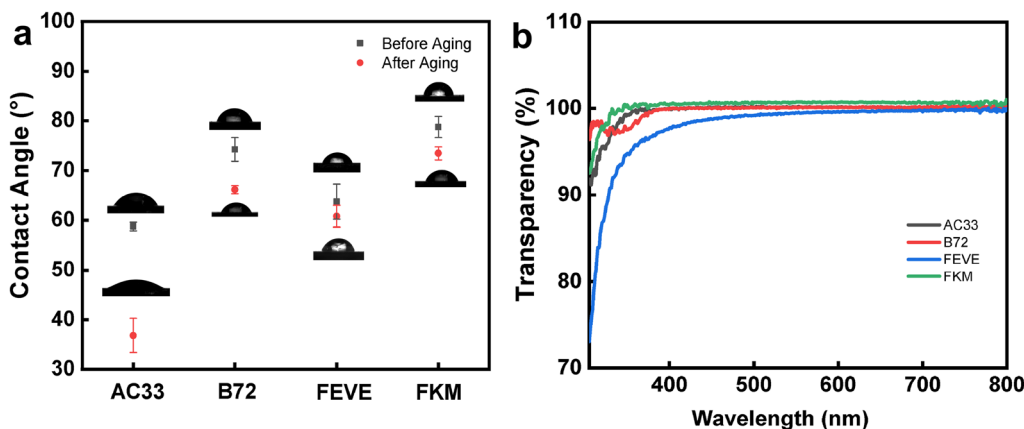


**Fig. 5** a Contact angles of the films before and after aging; b light transmittance of the four films

**Table 2** Pencil hardness of AC33, B72, FEVE, and FKM film samples, and tensile strength of samples made by coating reinforcement agents on the Xuan paper

Film Samples	Pencil hardness		Reinforcement agents applied on the Xuan paper	Tensile lap-shear strength (MPa)	
	Before degradation	After degradation		Before degradation	After degradation
AC33	HB	2B	AC33	6.37	5.00
B72	2H	H	B72	15.89	12.88
FEVE	H	F	FEVE	6.89	5.67
FKM	HB	B	FKM	4.71	3.55

in the reinforcement film can reduce the flexibility of the pigment layer, potentially leading to cracks. For instance, color paintings reinforced with B72 in the Puren Temple showed some cracking, as demonstrated in Fig. 2a<sub>2</sub>. This highlights a crucial balance between strength and flexibility in the choice of reinforcement materials for preserving the integrity of ancient paintings.

**Applications for model color painting samples**

To investigate how the reinforcing films affect the color performance of pigments, the optical properties of these pigments were evaluated both before and after the application of the four reinforcement materials. The procedure for preparing the reinforced model painting samples is shown in Fig. 6a, where pigment particles are visible prior to reinforcement (Fig. 6b). Figure 6c–f show the pigments after reinforcement, with the FKM solution demonstrating superior permeability into the pigment layer. In contrast, the other three reinforcing agents formed thicker films on the surface of the pigment layer. The effects of the coating materials on color changes of the pigment layer were then evaluated by color difference measurements, providing insights into how each

reinforcement material influences the visual aspects of the pigments.

The water vapor transmission property of the film determines the ability of the artifacts to exchange energy with the outside world after reinforcement, which is one of the important indicators to determine whether the reinforcement material can be used on the artifacts, and if the use of reinforcement materials leads to a reduction in water vapor transmission, which it might exacerbate peeling and detachment of the pigment layer. The four reinforcement films before and after 120-h UV degradation were prepared. In Fig. 6g, after keeping both undegraded and degraded four types of films still for 21 days, the water contents of undegraded AC33, B72, FEVE, and FKM films reduced by 4.31 g, 2.12 g, 3.72 g, and 2.52 g, and the water contents of the degraded films decreased by 5.2 g, 2.52 g, 4.22 g, and 3.82 g respectively. This indicates that although undegraded AC33 film presents the best permeability among all reinforcing materials, while the degraded AC33 film has the highest water loss among all reinforcing materials, which is consistent with the results of water contact angle measurement. Also, despite the relatively lower permeability of undegraded FEVE and FKM, the two reinforcing films demonstrate lower

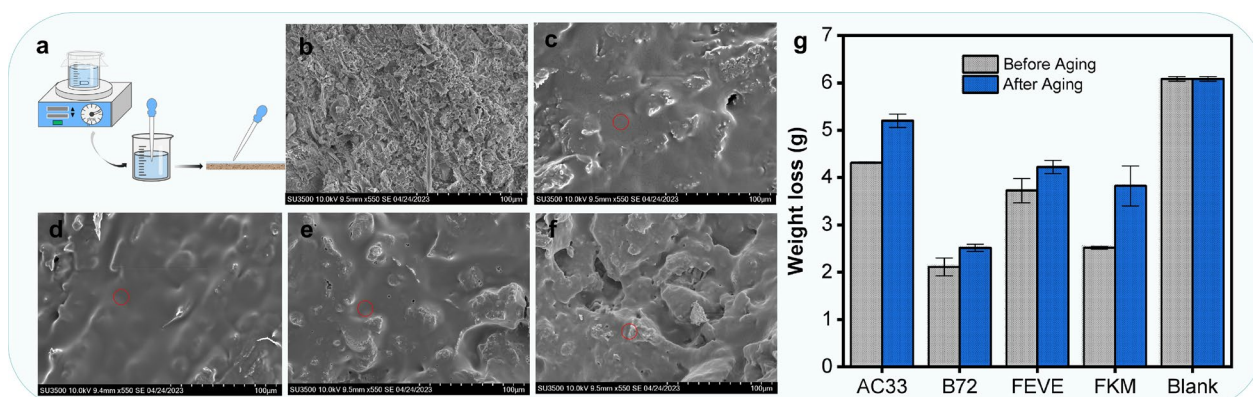


**Fig. 6** a Diagram of applying 1 mL reinforcement reagents on the model painting samples. SEM images of **b** the red pigment layer and the red pigment layer after coating with **c** AC33, **d** B72, **e** FEVE, and **f** FKM reagents, **g** water vapor transmission property of the films before and after aging

rates of water loss at 13.44% and 12.1% respectively, indicating good film durability.

In this study,  $\Delta E$  at 3 was used as the threshold to distinguish between obvious and non-obvious color differences [21, 50, 51]. The color changes in all six pigments, before and after reinforcement with the four materials, were found to be subtle. Further investigation was conducted on the color changes in both unreinforced and reinforced pigment layers, before and after 120-h UV degradation (Table 3). More than 80% of pigments reinforced with AC33, B72, and FKM present significant color changes after UV radiation ( $\Delta E > 3$ ). In contrast, the color differences in cinnabar, Paris green, and carbon black pigments before and after reinforcement with FEVE were minimal. Additionally, the films of AC33, FKM, and B72 did not significantly alter the color performance of carbon black. Unfortunately, all reinforcement materials used in this study cause a significant color change to orpiment, where B72 relatively leads to less color alteration.

Overall, a comprehensive assessment of the properties and durability of four widely used reinforcement agents,

i.e., AC33, B72, FKM, and FEVE, was carried out in this study, advantages and disadvantages of the four reinforcing materials were summarized in Table 4.

### Conclusions

In this study, in order to explore the applicability of mainly used reinforcement materials on different pigments, the properties and durability of AC33, B72, FKM, and FEVE agents were systematically evaluated, which are the reinforcement materials commonly used on paintings in ancient wooden architectures in four Chinese heritage institutions, and the following conclusions can be reached.

In summary, the films derived from the four reinforcement agents exhibit approximately 100% transmittance in the visible light spectra. Among them, the B72 film stands out as the most hydrophobic, showing superior reinforcing effects on carbon black. AC33 film has better permeability and fair tensile strength. On the other hand, the FKM film, while more hydrophobic, exhibits lower permeability and tensile strength. Notably, the FEVE film demonstrates the best overall properties, including enhanced hydrophobicity, higher permeability, and tensile strength compared to the others.

Our findings suggest that these four reinforcing agents are likely to be compatible with different pigments and specific application contexts. As explored in this study, the FKM material is more suitable to reinforce the lead white and Paris green, also, the better hydrophobicity of FKM film is more suitable for the reinforcement of color paintings stored in humid environments in southern China, and it can be used for color painting with lower damage degree due to its low tensile strength. The hydrophilic reinforcing film, i.e., AC33, can be used to conserve indoor color paintings. In addition, although the B72 film presents the highest tensile strength, it is particularly

**Table 3** Color difference ( $\Delta E$ ) of pigment layer, and pigment layer coated with AC33, B72, FEVE, and FKM reagents before and after 120-h UV degradation

Pigment layer	Pigment layer before reinforcement	Pigment layer after reinforcement			
		AC33	B72	FEVE	FKM
Lead white	7.25	7.06	6.10	4.75	3.56
Cinnabar	4.13	3.03	12.48	2.80	5.45
Ultramarine	11.97	16.90	4.36	7.21	12.50
Paris green	2.48	6.06	7.49	2.15	2.97
Orpiment	7.38	10.07	8.21	9.48	10.20
Carbon black	5.07	1.77	3.31	2.73	3.31

**Table 4** Advantages and drawbacks of the four reinforcing materials for color painting in ancient architecture

Reinforcing materials	Advantages	Drawbacks	Better reinforcing effect on pigments
B72	Better hydrophobicity Better transmittance	Lower permeability Excessive tensile strength Less smooth film	Carbon black
AC33	Better transmittance Better permeability Fair tensile strength Smooth film	Lower hydrophobicity	Carbon black, Cinnabar
FKM	Better hydrophobicity Better transmittance Less smooth film	Lower permeability Low tensile strength	Paris green, Lead white
FEVE	Better hydrophobicity Better transmittance Better permeability Fair tensile strength	Less smooth film	Cinnabar, Paris green, Carbon black

effective on severely damaged pigment layers. These insights provide valuable guidance for heritage conservators and curators in selecting the most appropriate reinforcement materials for practical application in the preservation of historical artworks.

#### Acknowledgements

This work was supported by the project of the Department of Ancient Architecture, Palace Museum.

#### Author contributions

Conceptualization, K.H.; and G.T.; resources, software, investigation, formal analysis. D.H.; methodology, data curation, C.C.; writing—original draft preparation, M.G.; and Y.T.; writing—review and editing, Y.L.; visualization, P.F.; supervision, project administration, and funding acquisition, Y.L.; All authors have read and agreed to the published version of the manuscript.

#### Funding

This work was supported by the National Cultural Heritage Administration of China. [Study on Conservation Effect Evaluation of Ancient Architecture Painting Technology]. Special thanks go to Fundamental Research Funds for the Central Universities (GK202304013) and Shaanxi Key Research and Development Program of China (2024GX-YBXM-560).

#### Availability of data and materials

The datasets used and/or analysis results obtained in the current study are available from the corresponding author on request.

#### Declarations

#### Competing interests

The authors declare that they have no competing financial interests.

Received: 4 February 2024 Accepted: 5 April 2024

Published online: 11 April 2024

#### References

- Han K, Yang H, Teri G, Hu S, Li J, Li Y, et al. Spectroscopic investigation of a color painting on an ancient wooden architecture from the Taiping Heavenly Kingdom Prince Dai's Mansion in Jiangsu China. *Minerals*. 2023. <https://doi.org/10.3390/min13020224>.
- Lei Z, Wu W, Shang G, Wu Y, Wang J. Study on colored pattern pigments of a royal Taoist temple beside the Forbidden City (Beijing, China). *Vib Spectrosc*. 2017;92:234–44. <https://doi.org/10.1016/j.vibspec.2017.08.005>.
- Shen AG, Wang XH, Xie W, Shen J, Li HY, Liu ZA, et al. Pigment identification of colored drawings from Wuying Hall of the Imperial Palace by micro-Raman spectroscopy and energy dispersive X-ray spectroscopy. *J Raman Spectrosc*. 2006;37:230–4. <https://doi.org/10.1002/jrs.1435>.
- Li Y, Wang F, Ma J, He K, Zhang M. Study on the pigments of Chinese architectural colored drawings in the Altar of Agriculture (Beijing, China) by portable Raman spectroscopy and ED-XRF spectrometers. *Vib Spectrosc*. 2021. <https://doi.org/10.1016/j.vibspec.2021.103291>.
- Wang N, He L, Zhao X, Simon S. Comparative analysis of eastern and western drying-oil binding media used in polychrome artworks by pyrolysis–gas chromatography/mass spectrometry under the influence of pigments. *Microchim J*. 2015;123:201–10. <https://doi.org/10.1016/j.microc.2015.06.007>.
- Fu P, Teri G-L, Li J, Li J-X, Li Y-H, Yang H. Investigation of ancient architectural painting from the Taidong tomb in the western qing tombs, hebei, china. *Coatings*. 2020;10:688. <https://doi.org/10.3390/coatings10070688>.
- Peifan Q, Deqi Y, Qi M, Aijun S, Jingqi S, Zengjun Z, et al. Study and restoration of the Yi Ma Wu Hui layer of the ancient coating on the Putuo Zongcheng Temple. *Int J Archit Herit*. 2021;15:1707–21. <https://doi.org/10.1080/15583058.2020.1719232>.
- Wang X, Zhen G, Hao X, Tong T, Ni F, Wang Z, et al. Spectroscopic investigation and comprehensive analysis of the polychrome clay sculpture of Hua Yan Temple of the Liao Dynasty. *Spectrochim Acta Part A Mol Biomol Spectrosc*. 2020;240:118574. <https://doi.org/10.1016/j.saa.2020.118574>.
- Chen E, Zhang B, Zhao F, Wang C. Pigments and binding media of polychrome relics from the central hall of Longju temple in Sichuan, China. *Herit Sci*. 2019;7:1–8. <https://doi.org/10.1186/s40494-019-0289-3>.
- Schifano E, Cavallini D, De Bellis G, Bracciale MP, Felici AC, Santarelli ML, et al. Antibacterial effect of zinc oxide-based nanomaterials on environmental biodeteriogens affecting historical buildings. *Nanomaterials*. 2020;10:335. <https://doi.org/10.3390/nano10020335>.
- Teri G, Fu P, Han K, Li J, Li Y, Jia Z, et al. Color paintings of Taiping Heavenly Kingdom royal residence: an analytical study. *Coatings*. 2022;12:1880. <https://doi.org/10.3390/coatings12121880>.
- Ntelia E, Karapanagiotis I. Superhydrophobic paraloid B72. *Prog Org Coat*. 2020;139: 105224. <https://doi.org/10.1016/j.porgcoat.2019.105224>.
- Zhang Y, Li X, Zhu J, Wang S, Wei B. Hybrids of CNTs and acrylic emulsion for the consolidation of wall paintings. *Prog Org Coat*. 2018;124:185–92. <https://doi.org/10.3390/nano8090649>.
- Carretti E, Dei L. Physicochemical characterization of acrylic polymeric resins coating porous materials of artistic interest. *Prog Org Coat*. 2004;49:282–9. <https://doi.org/10.1016/j.porgcoat.2003.10.011>.
- Cocca M, D'ariento L, D'orazio L, Gentile G, Martuscelli E. Polyacrylates for conservation: chemico-physical properties and durability of different commercial products. *Polym Testing*. 2004;23:333–42. [https://doi.org/10.1016/S0142-9418\(03\)00105-3](https://doi.org/10.1016/S0142-9418(03)00105-3).
- Li Y, Zhao L. Characterization, property and application of PVAc emulsion as a kind of conservation material for painted cultural relics. *Sci Conserv Archaeol*. 2021;33:22–32. <https://doi.org/10.16334/j.cnki.cn31-1652/k.20201201987>.
- Zhou Y. Study on the application of five kinds of conservation materials in the conservation of red sandstone relics in Guangdong region. *Hakka Cultural Heritage Vision*. 2016:45–9.
- Yang X, Xu F. Detection and protection of painted wood parts of Yanzong Temple in Yangzhou. *Relics Museol*. 2022:88-95 (in Chinese with english abstract).
- Masi G, Bernardi E, Martini C, Vassura I, Sklep L, Švara Fabjan E, et al. An innovative multi-component fluoropolymer-based coating on outdoor patinated bronze for cultural heritage: durability and reversibility. *J Cult Herit*. 2020;45:122–34. <https://doi.org/10.1016/j.culher.2020.04.015>.
- Xu J, Jiang Y, Zhang T, Dai Y, Yang D, Qiu F, et al. Fabrication of UV-curable waterborne fluorinated polyurethane-acrylate and its application for simulated iron cultural relic protection. *J Coat Technol Res*. 2018;15:535–41. <https://doi.org/10.1007/s11998-017-0009-4>.
- Fu P, Teri G-L, Chao X-L, Li J, Li Y-H, Yang H. Modified graphene-FEVE composite coatings: application in the repair of ancient architectural color paintings. *Coatings*. 2020;10:1162. <https://doi.org/10.3390/coatings10121162>.
- Baglioni P, Berti D, Bonini M, Carretti E, Dei L, Fratini E, et al. Micelle, microemulsions, and gels for the conservation of cultural heritage. *Adv Colloid Interface Sci*. 2014;205:361–71. <https://doi.org/10.1016/j.cis.2013.09.008>.
- Giorgi R, Baglioni M, Berti D, Baglioni P. New methodologies for the conservation of cultural heritage: micellar solutions, microemulsions, and hydroxide nanoparticles. *Acc Chem Res*. 2010;43:695–704. <https://doi.org/10.1021/ar900193h>.
- Yang Y, Lian X, Yang Z, Zhou Y, Zhang X, Wang Y. Self-shaping microemulsion gels for cultural relic cleaning. *Langmuir*. 2021;37:11474–83. <https://doi.org/10.1021/acs.langmuir.1c01649>.
- Alberghina MF, Barraco R, Basile S, Brai M, Pellegrino L, Prestileo F, et al. Mosaic floors of roman Villa del Casale: principal component analysis on spectrophotometric and colorimetric data. *J Cult Herit*. 2014;15:92–7. <https://doi.org/10.1016/j.culher.2012.12.004>.
- Alonso-Villar E, Rivas T, Pozo-Antonio J. Adhesives applied to granite cultural heritage: effectiveness, harmful effects and reversibility. *Constr Build Mater*. 2019;223:951–64. <https://doi.org/10.1016/j.conbuildmat.2019.08.010>.
- Molina MT, Salvadori B, Cano E, de la Fuente D, Ramírez-Barat B. Exploration of coating alternatives for the protection of bare steel and brass in scientific-technical artefacts. *Herit Sci*. 2023;11:1–15. <https://doi.org/10.1186/s40494-023-01049-5>.



28. Unoki M, Kimura I, Yamauchi M. Solvent-soluble fluoropolymers for coatings—chemical structure and weatherability. *Surf Coat Int Pt B Coat Trans.* 2002;85:209–13. <https://doi.org/10.1007/bf02699511>.
29. Zhong B, Shen L, Zhang X, Li C, Bao N. Reduced graphene oxide/silica nanocomposite-reinforced anticorrosive fluorocarbon coating. *J Appl Polym Sci.* 2021;138:49689. <https://doi.org/10.1002/app.49689>.
30. Mazzola M, Frediani P, Bracci S, Salvini A. New strategies for the synthesis of partially fluorinated acrylic polymers as possible materials for the protection of stone monuments. *Eur Polymer J.* 2003;39:1995–2003. [https://doi.org/10.1016/s0014-3057\(03\)00110-1](https://doi.org/10.1016/s0014-3057(03)00110-1).
31. Malshe VC, Sangaj NS. Fluorinated acrylic copolymers. *Prog Org Coat.* 2005;53:207–11. <https://doi.org/10.1016/j.porgcoat.2005.03.003>.
32. Rutter T, Hutton-Prager B. Investigation of hydrophobic coatings on cellulose-fiber substrates with in-situ polymerization of silane/siloxane mixtures. *Int J Adhes Adhes.* 2018;86:13–21. <https://doi.org/10.1016/j.ijadhadh.2018.07.008>.
33. Soytürk EE, Kartal SN, Terzi E, Nses MS, Arkdemir K, Elik N. Evaluation of wood treated with Paraloid B72 and boric acid: thermal behavior, water absorption and mold resistance. *Eur J Wood Wood Prod.* 2023;81:923–34.
34. Chelazzi D, Poggi G, Jaidar Y, Toccafondi N, Giorgi R, Baglioni P. Hydroxide nanoparticles for cultural heritage: Consolidation and protection of wall paintings and carbonate materials. *J Colloid Interface Sci.* 2013;392:42–9.
35. Fang S, Zhang K, Zhang H, Zhang B. A study of traditional blood lime mortar for restoration of ancient buildings. *Cem Concr Res.* 2015;76:232–41. <https://doi.org/10.1016/j.cemconres.2015.06.006>.
36. Lin H, Lourenço SD, Yao T, Zhou Z, Yeung A, Hallett P, et al. Imparting water repellency in completely decomposed granite with Tung oil. *J Clean Prod.* 2019;230:1316–28. <https://doi.org/10.1016/j.jclepro.2019.05.032>.
37. Yang W, Xiao D. The protection and effect of ancient architecture painting in Shanshan Guild Hall, Luoyang. *Traditional Chinese Architecture and Gardens.* 2011;No.113:26–8+5+84 (in Chinese).
38. Luo Y, Cigić IK, Wei Q, Marinšek M, Strlič M. Material properties and durability of 19th–20th century Tibetan manuscripts. *Cellulose.* 2023;30:11783–95. <https://doi.org/10.1007/s10570-023-05631-9>.
39. Mistretta MC, La Mantia FP, Titone V, Megna B, Botta L, Morreale M. Durability of biodegradable polymers for the conservation of cultural heritage. *Front Mater.* 2019. <https://doi.org/10.3389/fmats.2019.00151>.
40. Bourguignon E, Tomasin P, Detalle V, Vallet J-M, Labouré M, Olteanu I, et al. Calcium alkoxides as alternative consolidants for wall paintings: evaluation of their performance in laboratory and on site, on model and original samples, in comparison to conventional products. *J Cult Herit.* 2018;29:54–66. <https://doi.org/10.1016/j.culher.2017.07.008>.
41. Ibrahim MM, Mohamed SO, Hefni YK, Ahmed AI. Nanomaterials for consolidation and protection of Egyptian faience form Matteria, Egypt. *J Nano Res.* 2019;56:39–48. <https://doi.org/10.4028/www.scientific.net/JNanoR.56.39>.
42. Li W, Lin J, Zhao Y, Pan Z. The adverse effects of TiO<sub>2</sub> photocatalycity on paraloid B72 hybrid stone relics protective coating aging behaviors under UV irradiation. *Polymers.* 2021;13:262. <https://doi.org/10.3390/polym13020262>.
43. Gennes P-G, Brochard-Wyart F, Quéré D. Capillarity and wetting phenomena: drops, bubbles, pearls, waves. Berlin: Springer; 2004.
44. Helmi FM, Hefni YK. A simple method for measuring the static water contact angle for evaluation the hydrophobicity of the consolidating and protective materials. 2014.
45. Melki S, Biguenet F, Dupuis D. Hydrophobic properties of textile materials: robustness of hydrophobicity. *J Textile Inst.* 2019;110:1221–8. <https://doi.org/10.1080/00405000.2018.1553346>.
46. Wang Y. Synthesis and properties of photo-cross-linkable functional fluoroelastomers [In Chinese with English Abstract]. Harbin Inst Technol. 2021. <https://doi.org/10.27061/d.cnki.ghgdu.2019.005851>.
47. Lin Z, Cheng Y, Lü H, Zhang L, Yang B. Preparation and characterization of novel ZnS/sulfur-containing polymer nanocomposite optical materials with high refractive index and high nanophase contents. *Polymer.* 2010;51:5424–31. <https://doi.org/10.1016/j.polymer.2010.09.017>.
48. Xu L, Geng Z, He J, Zhou G. Mechanically robust, thermally stable, broadband antireflective, and superhydrophobic thin films on glass substrates. *ACS Appl Mater Interfaces.* 2014;6:9029–35. <https://doi.org/10.1021/am5016777>.
49. Resetco C, Dikić T, Verbrugge T, Du Prez FE. UV-cured multifunctional coating resins prepared from renewable thiolactone derivatives. *Prog Org Coat.* 2017;107:75–82. <https://doi.org/10.1016/j.porgcoat.2016.11.030>.
50. Cui X. Study on anti-weathering reinforcement of sandstone quality painting in Zichang Zhongshan Grottoes [Master]. Shaanxi Normal Univ. 2022. <https://doi.org/10.27292/d.cnki.gsxfu.2022.000038>.
51. Mao T, Li X, Shi X, Hu Y, Zha J, Luo X, et al. Study on the performance of acrylic polyurethane for the protection of handwriting on paper relics. *Coatings.* 2023;13:822. <https://doi.org/10.3390/coatings13050822>.

## Publisher's Note

Springer Nature remains neutral with regard to jurisdictional claims in published maps and institutional affiliations.